



ELSEVIER

Contents lists available at ScienceDirect

Materials Letters

journal homepage: www.elsevier.com/locate/matlet

Study on the elastic–plastic behavior of a porous hierarchical bioscaffold used for bone regeneration



Shiping Huang^a, Zhiyong Li^b, Zhou Chen^a, Qiang Chen^{b,*}, Nicola Pugno^{c,d,*}

^a School of Civil Engineering and Transportation, South China University of Technology, Guangzhou 510640, PR China

^b Biomechanics Laboratory, School of Biological Science and Medical Engineering, Southeast University, Nanjing 210096, PR China

^c Laboratory of Bio-Inspired & Graphene Nanomechanics, Department of Civil, Environmental and Mechanical Engineering, University of Trento, 38123 Trento, Italy

^d Center for Materials and Microsystems, Fondazione Bruno Kessler, Via Sommarive 18, 38123 Povo (Trento), Italy

ARTICLE INFO

Article history:

Received 22 May 2013

Accepted 25 August 2013

Available online 31 August 2013

Keywords:

Bone regeneration

Hierarchical scaffold

Mechanical properties

Porosity

Elastic–plastic behavior

ABSTRACT

A perfectly plastic von Mises model is proposed to study the elastic–plastic behavior of a porous hierarchical scaffold used for bone regeneration. The proposed constitutive model is implemented in a finite element (FE) routine to obtain the stress–strain relationship of a uniaxially loaded cube of the scaffold, whose constituent is considered to be composed of cortical bone. The results agree well with experimental data for uniaxial loading case of a cancellous bone. We find that the unhomogenized stress distribution results in different mechanical properties from but still comparable to our previous theory. The scaffold is a promising candidate for bone regeneration.

© 2013 Elsevier B.V. All rights reserved.

1. Introduction

Bioscaffolds should provide sufficient mechanical support and pore–gradient structures where cells can adhere, migrate, differentiate etc. Thus, porous scaffolds have attracted much attention and are considered as promising candidates for tissue regeneration [1]. From the viewpoint of the mechanics of natural materials, the high strength, stiffness and toughness of bone have been clearly linked to its hierarchical structure [2]; it follows that a hierarchical structure of a porous scaffold would be ideally suited to its function of allowing bone regeneration while supporting applied loads [3].

To this end, a number of researchers have experimented with a variety of hierarchical scaffolds to mimic the structure of bone and studied their ability to support bone formation. Liao et al. [4] developed a hierarchical scaffold and studied its bioactivity based on HA/collagen/PLA composite; Jones et al. [3] developed a hierarchical scaffold made of bioactive glass at the molecular scale to optimize its fusion with surrounding bone tissue. However, the mechanical properties of these scaffolds were not investigated broadly. On the other hand, since bone is an anisotropic, visco-elastic–plastic material, its mechanical behavior is not easy to be analytically characterized. Correspondingly, micromechanics [5–7] and Finite Element Analysis (FEA) [8,9] are often used to model the

mechanical properties (stiffness and strength), the elastic stress and strain fields of bone scaffolds. In these models, geometric models of porous scaffolds are often reconstructed by image technology [9], such as Micro–CT [8]. And the quantitative analysis based on the micromechanics and FEA is helpful to understand the mechanical stimuli on cells [9], dissolution rate on bone regeneration [10] and local stress distribution [7] in the scaffold.

In our previous work, we proposed a hierarchical scaffold model using a bottom–up method reported in Ref. [11] and developed a theoretical framework to calculate the scaffold's Young's modulus and strength [1]. In this letter, we focus on the elastic–plastic behavior of the proposed hierarchical scaffold model (Fig. 1). By considering the solid matrix of the scaffold to be bovine cortical bone, the stress–strain curves of the one–level and two–level scaffold models with different porosities are generated. In particular, selected curves for each model are compared with the experimental result of a bovine cancellous bone [12], and the overall material properties obtained from FEA are compared with the theoretical results from our previous work.

2. Elastic–plastic modeling of the scaffold

The geometry of the one–level unit cell is represented by a cube (side length $2a^{(1)}$) from which a sphere (radius $R^{(1)}$), with the same centroid, is subtracted, as seen in Fig. 1(b); the two–level unit cell is composed of $n \times n \times n$ one–level unit cells (side length $2a^{(2)} = n \times 2a^{(1)}$), then another sphere (radius $R^{(2)}$) with the same

* Corresponding authors. Tel./fax: +86 25 83792620.

E-mail addresses: chenq999@gmail.com (Q. Chen), nicola.pugno@unitn.it (N. Pugno).

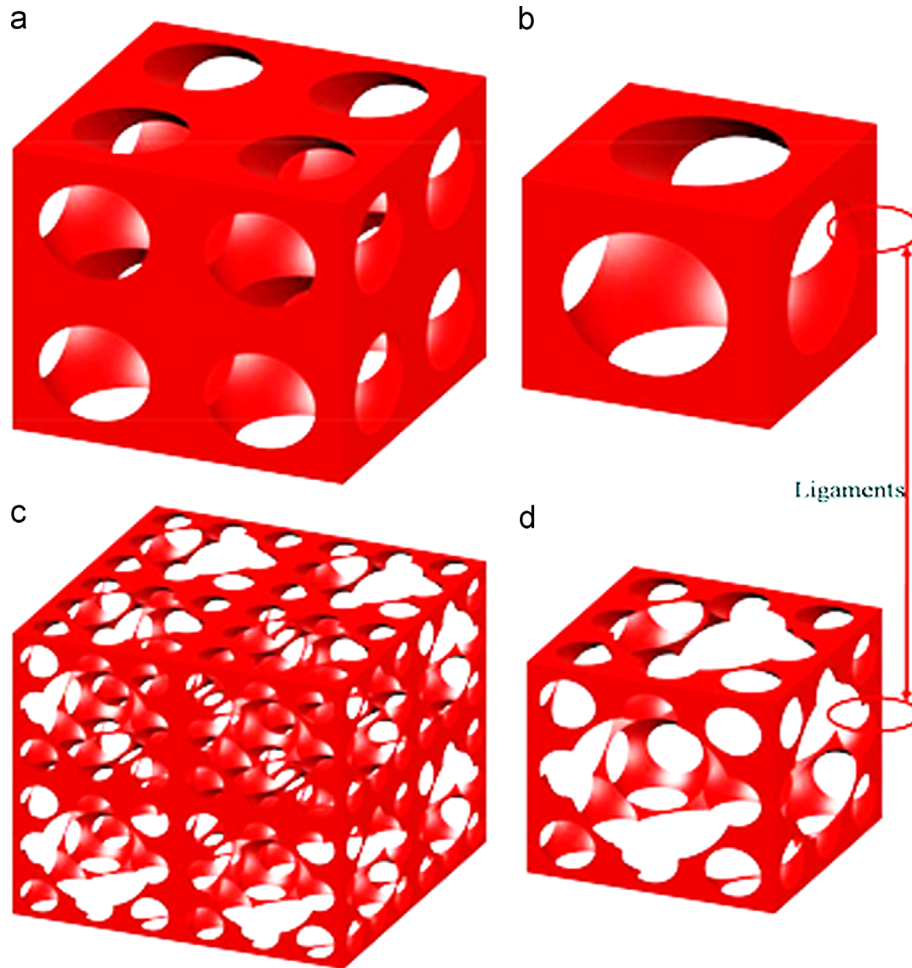


Fig. 1. Schematic of the hierarchical porous scaffold model. (a) One-level model; (b) unit cell of the one-level model; (c) two-level model; (d) unit cell of the two-level model.

centroid (Fig. 1b) is subtracted from it, and so on until the k -level unit cell. It is noted that $a^{(k)}$ and $R^{(k)}$ must meet the condition $\sqrt{2}/2 < a^{(k)}/R^{(k)} < 1$ in order to form interconnecting pores for cellular activity. The gross area of the k -level unit cell is $A^{(k)} = 4(a^{(k)})^2$. The one-level unit cell porosity can be expressed as $p^{(1)} = V_p^{(1)}/V_u^{(1)}$, where $V_p^{(1)}$ and $V_u^{(1)}$ are the pore volume inside the unit cell and the unit cell volume, respectively. For the one-level and two-level unit cells shown in Fig. 1, the porosity $p^{(1)}$ and $p^{(2)}$ are in the range of 52.4% to 96.5% and 75.5% to 99.7% [1], respectively. For the k -level self-similar structure, its porosity can be approximately expressed as $p^{(k)} = 1 - (1 - p^{(1)})^k$. The precise calculations for the porosity and the varying cross-sectional area are given in the Supplemental Material.

As mentioned in Introduction, we assume the cortical bone to be the constituent material of the scaffold. According to Johnson et al. [13], the cortical bone exhibits a visco-elastic-plastic behavior under different strain rates. They showed that at extremely low rates only the elastic and viscoplastic portions of the model contribute to the overall stress-strain response of the material [13], which is close to the elastic perfectly plastic behavior. Thus, the loading here is considered to be done at extremely low strain rate, and the constituent materials' behavior is simplified to be rate-independent elastic perfectly plastic. Then, the yield function f in the stress space is given as $f(\sigma_{ij}) = (\sigma_{ij} - \sigma_m \delta_{ij})(\sigma_{ji} - \sigma_m \delta_{ji})/2 = \sigma_s^2/3$, where σ_{ij} is the stress tensor, δ_{ij} is the Kronecker delta, σ_m is the mean stress (i.e., $\sigma_m = \delta_{ij}/3$) and σ_s is the yield stress in uniaxial loading test. In the plastic stage, the loads are discretized into finite increments, and for each increment, the constitutive behavior is

considered to be linear. Based on the plasticity theory, the detailed derivation of the incremental elastic-plastic constitutive equation is given in the Supplemental Material. In order to get the structure's response, a uniform displacement Δ is applied on its top surface until the structure fails and the corresponding reaction force F is obtained. For the k -level unit cell, the structure's Young's modulus and strength are calculated by $E^{(k)} = F/(2a^{(k)}\Delta)$ and $\sigma_y^{(k)} = F_y^{(k)}/A^{(k)}$, respectively, where $F_y^{(k)}$ is the force when the scaffold begins to yield.

3. Results and discussion

In FE models, the one-level model is formed by a $3 \times 3 \times 3$ one-level unit cell, while the two-level model is a two-level unit cell composed of $3 \times 3 \times 3$ one-level cells. The basic mechanical constants of the bovine cortical bone are $E_s = 15$ GPa [13], $\sigma_s = 225$ MPa [14] and $\nu_s = 0.3$, which is an intermediate value according to Rupin et al. [15].

3.1. Constitutive behavior of the scaffold material

In order to demonstrate the elastic-plastic behavior of the scaffolds under different porosities, nine parametric study cases have been presented (Fig. 2a and b). In Fig. 2, we can see that the plateau regime and the slope of the linear-elastic phase (i.e., structure's Young's modulus) decrease as the porosity increases, this is because increasing porosity results in a thinner ligament (Fig. 1b and d). Moreover, Fig. 2c shows a good agreement between

the two models and experiments; it is worth mentioning that there is a slight difference between the porosity (0.84) of the one-level scaffold, which is higher than that (0.81) of the two-level one, however, the two-level scaffold has a porosity gradient, which makes it a better candidate for fractal-like angiogenesis [16] or transport of nutrients from nano-/micro- to macro-scale due to superior biological functionality.

As an example, the stress nephogram of the two cases in Fig. 2c are shown in Fig. 3. The porosity of the one-level model is 0.84 and that of the two-level model is 0.81. Fig. 3 shows that the stress concentration phenomenon apparently exists in the whole structure. In order to observe the elastic–plastic stress state of any location, a stress state ratio is defined as $f/(\sigma_s^2/3)$, where f is the trial

stress function. If the ratio is greater than unity, it implies that the point deforms plastically, otherwise, the point deforms elastically. Moreover, the yielding point always begins at the minimum cross-sectional area location where cells will receive the strongest mechanical stimulus.

3.2. Structure's Young's modulus and strength

The structure's Young's modulus $E^{(k)}$ and strength $\sigma_y^{(k)}$ can be calculated by the formula introduced in Section 2. As demonstrated by the FEA results in Fig. 4, the structure's stiffness and strength decrease as the porosity increases in both structures. It can be also seen that the FEA results show a quasi-linear dependence of

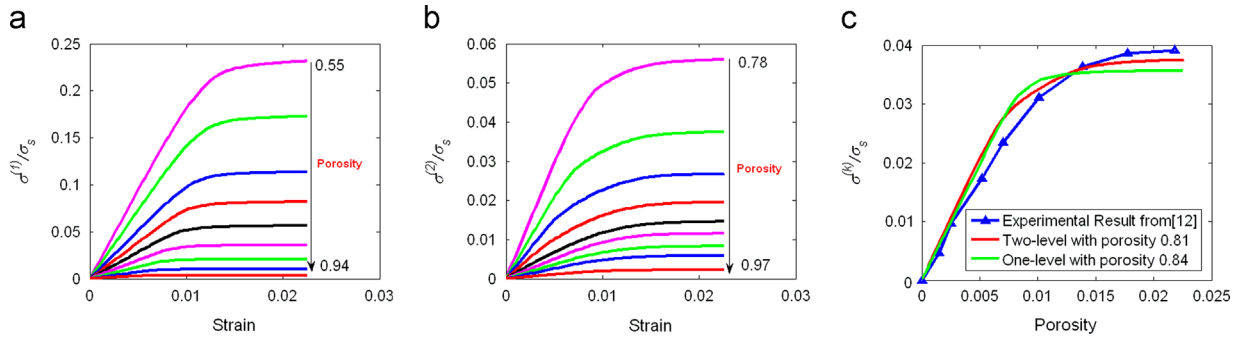


Fig. 2. Stress–strain relationship under different porosity: (a) One-level scaffold, (b) two-level scaffold, (c) comparison between experimental result of the cancellous bone from [12], one-level and two-level models.

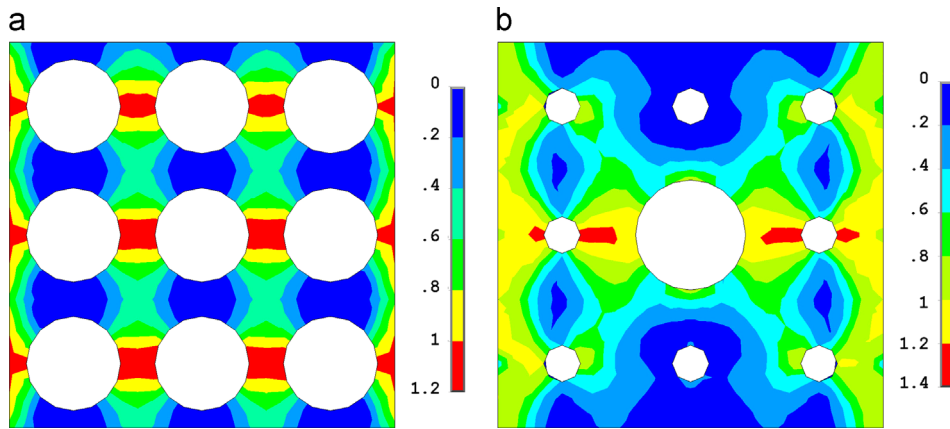


Fig. 3. (a) Stress nephogram of the one-level model; (b) stress nephogram of the two-level model.

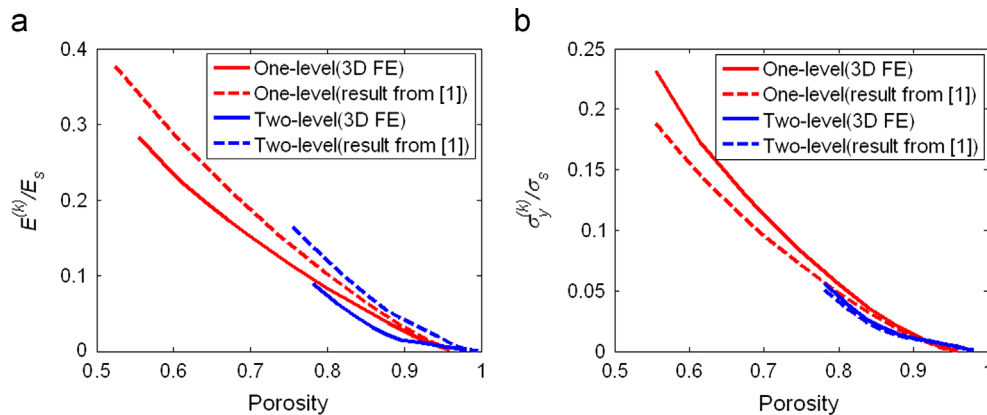


Fig. 4. Comparison of the structure Young's modulus with prediction [1]: (a) Porosity vs. structure's Young's modulus, (b) Porosity vs. structure's strength. (For interpretation of the references to color in this figure legend, the reader is referred to the web version of this article.)

structure's stiffness and strength on porosity (corresponding correlation coefficient are 0.994 and 0.988) for the one-level scaffold, which is confirmed by the micromechanical approaches [6–18], while this relationship is not so clear for the two-level scaffold. In particular, for the one-level structure, its normalized Young's modulus ratio $E^{(1)}/E_s$ varies from 0.283 to 0.001 (the red solid line in Fig. 4a; i.e., 4245 MPa to 15 MPa for $E^{(1)}$) as the porosity increases from 0.55 to 0.94; while the normalized Young's modulus $E^{(2)}/E_s$ of the two-level structure varies from 0.089 to 0.002 (the blue solid line in Fig. 4a; i.e., 1335 MPa to 30 MPa for $E^{(2)}$) as the porosity increases from 0.78 to 0.94. The strength of the structure follows a similar trend. The normalized strength of the one-level structure $\sigma_y^{(1)}/\sigma_s$ decreases from 0.23 to 0.004 (the red solid line in Fig. 4b; i.e., 52.75 MPa to 0.9 MPa for $\sigma_y^{(1)}$) as the porosity varies from 0.55 to 0.94; and the normalized strength of the two-level structure $\sigma_y^{(2)}/\sigma_s$ decreases from 0.056 to 0.002 (the blue solid line in Fig. 4b; i.e., 12.60 MPa to 0.45 MPa for $\sigma_y^{(2)}$) as the porosity varies from 0.78 to 0.94. These results are comparable to the data provided by Hayes et al. [19], who reported the ranges of the Young's modulus and strength of the cancellous bone are from 10 MPa to 1000 MPa and 0.1 to 100 MPa, respectively. The FE results match the trends of the theoretical results in the author's previous work [1], see Fig. 4. But there exists a difference between them, in that the unhomogenized stress distribution in the structures, which is not considered in Ref. [1], is clearly shown in the FE results. It is noted that the bone exhibits an anisotropic nature both in the extracellular bone matrix and the morphology of the intertrabecular pores [20,21]. The former determines the micromechanical behavior of trabeculae, which can predict the mechanical properties of trabecular bone [20]. As for anisotropic morphology, bone is often modeled as a transversely isotropic material. In this regard, the current scaffold model can be easily extended to model the anisotropic morphology by replacing the spherical pores with ellipsoidal pores.

4. Conclusions

The stress–strain relationships of the one-level and two-level porous hierarchical scaffolds are parametrically studied using FE modeling, and the results at close porosities agree well with the experimental result of the cancellous bone from literature. Besides, the basic mechanical properties, i.e. Young's modulus and strength are compared with those of the author's theoretical work and there exists a difference due to the unhomogenized stress distribution in the structures. Finally, the scaffold model has been shown to be a promising candidate for bone tissue regeneration.

Acknowledgements

Qiang Chen is supported by Scientific Research Starting Foundation "Study on the Mechanical Properties of Biodegradable Hierarchical Scaffolds in Bone Tissue Engineering", Southeast University. Shipping Huang would like to acknowledge the support from the Fundamental Research Funds for the Central Universities, Grant No.2012ZB0024. This work is also supported by the ERC Ideas Starting Grant No. 279985 'BIHSNAM—Bio-Inspired Hierarchical Super Nanomaterials' (PI Nicola Pugno) and ERC Proof of Concept REPLICA (PI Nicola Pugno).

Appendix A. Supplementary material

Supplementary data associated with this article can be found in the online version at <http://dx.doi.org/10.1016/j.matlet.2013.08.114>.

References

- [1] Chen Q, Huang S. Mechanical properties of a porous bioscaffold with hierarchy. *Materials Letters* 2013;95:89–92.
- [2] Zimmermann EA, Schaible E, Bale H, Barth HD, Tang SY, Reichert P, et al. Age-related changes in the plasticity and toughness of human cortical bone at multiple length scales. *Proceedings of the National Academy of Sciences of the United States of America* 2011;108:14416–21.
- [3] Jones JR, Lee PD, Hench LL. Hierarchical porous materials for tissue engineering. *Philosophical Transactions of the Royal Society of London, Series A* 2006;364:263–81.
- [4] Liao S, Cui F, Zhang W, Feng Q. Hierarchically biomimetic bone scaffold materials: nano-HA/collagen/PLA composite. *Journal of Biomedical Materials Research Part B Applied Biomaterials* 2004;69:158–65.
- [5] Bertrand E, Hellmich C. Multiscale elasticity of tissue engineering scaffolds with tissue-engineered bone: a continuum micromechanics approach. *Journal of Engineering Mechanics-ASCE* 2009;135:395–412.
- [6] Fritsch A, Dormieux L, Hellmich C, Sanahuja J. Mechanical behavior of hydroxyapatite biomaterials: an experimentally validated micromechanical model for elasticity and strength. *Journal of Biomedical Materials Research Part A* 2009;88:149–61.
- [7] Scheiner S, Sinibaldi R, Pichler B, Komlev V, Renghini C, Vitale-Brovarone C, et al. Micromechanics of bone tissue-engineering scaffolds, based on resolution error-cleared computer tomography. *Biomaterials* 2009;30:2411–9.
- [8] Dejaco A, Komlev VS, Jaroszewicz J, Swieszkowski W, Hellmich C. Micro CT-based multiscale elasticity of double-porous (pre-cracked) hydroxyapatite granules for regenerative medicine. *Journal of Biomechanics* 2012;45:1068–75.
- [9] Lacroix D, Chateau A, Ginebra M-P, Planell JA. Micro-finite element models of bone tissue-engineering scaffolds. *Biomaterials* 2006;27:5326–34.
- [10] Byrne DP, Lacroix D, Planell JA, Kelly DJ, Prendergast PJ. Simulation of tissue differentiation in a scaffold as a function of porosity, Young's modulus and dissolution rate: application of mechanobiological models in tissue engineering. *Biomaterials* 2007;28:5544–54.
- [11] Chen Q, Pugno NM. Modeling the elastic anisotropy of woven hierarchical tissues. *Composites Part B Engineering* 2011;42:2030–7.
- [12] Guillén T, Zhang Q-H, Tozzi G, Ohrndorf A, Christ H-J, Tong J. Compressive behaviour of bovine cancellous bone and bone analogous materials, microCT characterisation and FE analysis. *Journal of the Mechanical Behavior of Biomedical Materials* 2011;4:1452–61.
- [13] Johnson T, Socrate S, Boyce M. A viscoelastic, viscoplastic model of cortical bone valid at low and high strain rates. *Acta Biomaterialia* 2010;6:4073–80.
- [14] Ferreira F, Vaz M, Simoes J. Mechanical properties of bovine cortical bone at high strain rate. *Materials Characterization* 2006;57:71–9.
- [15] Rupin F, Saied A, Dalmas D, Peyrin F, Hauptert S, Barthel E, et al. Experimental determination of Young modulus and Poisson ratio in cortical bone tissue using high resolution scanning acoustic microscopy and nanoindentation. *Journal of the Acoustical Society of America* 2008;123:3785.
- [16] Burri PH, Djonov V. Intussusceptive angiogenesis—the alternative to capillary sprouting. *Molecular Aspects of Medicine* 2002;23:1–27.
- [17] Fritsch A, Hellmich C, Dormieux L. Ductile sliding between mineral crystals followed by rupture of collagen crosslinks: experimentally supported micromechanical explanation of bone strength. *Journal of Theoretical Biology* 2009;260:230–52.
- [18] Hellmich C, Ulm F-J, Dormieux L. Can the diverse elastic properties of trabecular and cortical bone be attributed to only a few tissue-independent phase properties and their interactions? *Biomechanics and Modeling in Mechanobiology* 2004;2:219–38.
- [19] Hayes WC, Piazza S, Zysset P. Biomechanics of fracture risk prediction of the hip and spine by quantitative computed tomography. *Radiologic Clinics of North America* 1991;29:1–18.
- [20] Kabel J, Van Rietbergen B, Odgaard A, Huiskes R. Constitutive relationships of fabric, density, and elastic properties in cancellous bone architecture. *Bone* 1999;25:481–6.
- [21] Malandrino A, Fritsch A, Lahayne O, Kropik K, Redl H, Noailly J, et al. Anisotropic tissue elasticity in human lumbar vertebra, by means of a coupled ultrasound-micromechanics approach. *Materials Letters* 2012;78:154–8.